

## Voltage clamp studies on S-layer-supported tetraether lipid membranes

Bernhard Schuster, Dietmar Pum, Uwe B. Sleytr \*

Center for Ultrastructure Research and Ludwig Boltzmann-Institute for Molecular Nanotechnology, Universität für Bodenkultur Wien,  
Gregor Mendel Straße 33, A-1180 Vienna, Austria

Received 12 June 1997; revised 15 August 1997; accepted 18 August 1997

### Abstract

Isolated subunits from the cell surface proteins (S-layer) of *Bacillus coagulans* E38-66 have been recrystallized on a glycerol dialkyl nonitol tetraether lipid (GDNT)-monolayer and the electrophysical features of this biomimetic membrane have been investigated in comparison to unsupported GDNT-monolayers. The GDNT-monolayer, spread on a Langmuir–Blodgett trough, was clamped with the tip of a glass patch pipette. In order to investigate the barrier function and potential to incorporate functional molecules, voltage-clamp examinations on plain and S-layer-supported GDNT-monolayers were performed. Our results indicate the formation of a tight GDNT-monolayer sealing the tip of the glass pipette, and a decrease in conductance of the GDNT-monolayer upon recrystallization of the S-layer protein. Thus, the S-layer protein, apparently, did not penetrate or rupture the lipid monolayer. The valinomycin-mediated increase in conductance was less pronounced for the S-layer-supported than for the plain GDNT-monolayer, indicating differences in the accessibility and/or in the fluidity of the lipid membranes. Furthermore, in contrast to plain GDNT-monolayers, S-layer supported GDNT-monolayers with high valinomycin-mediated conductance persisted over long periods of time, indicating enhanced stability. These composite S-layer/lipid films may constitute a new tool for electrophysical and electrophysiological studies on membrane-associated and membrane-integrated biomolecules. © 1998 Elsevier Science B.V.

**Keywords:** Crystalline surface (S)-layer; Tetraether lipid monolayer; Valinomycin; Electron microscopy; Biomimetic membrane

### 1. Introduction

Two-dimensional crystalline cell surface layers, referred to as S-layers [1,2] are one of the most commonly observed outermost cell envelope components in bacteria. They are composed of single protein or glycoprotein species with molecular weights ranging from 40 000 to 200 000 [3,4]. S-layers can exhibit either oblique, square or hexagonal lattice symmetry with spacings of the morphological units in

the 3–30 nm range [2,4,5]. With respect to their inner and outer faces, S-layers are highly anisotropic with regard to their topography [6–8] and physicochemical properties [7,9,10]. S-layer lattices are structures with pores of identical size and morphology in the 2–5 nm range [9,11].

The S-layer from *Bacillus coagulans* E38-66, used in the present study, represents a highly specialized supramolecular structure. The characteristic features can be summarized as follows:

1. composed of identical, nonglycosylated protein subunits ( $M_r$  of 100 000);
2. oblique lattice symmetry with lattice constants of  $a = 9.4$  nm,  $b = 7.4$  nm, and base angle  $\gamma = 80^\circ$ ;

\* Corresponding author. Fax: +43-1-4789112; E-mail: sleytr@edv1.boku.ac.at

3. a thickness of  $\sim 5$  nm;
4. anisotropic topographical surface properties;
5. very precise molecular sieving properties due to charge-neutral 3.5 nm diameter pores, preventing unspecific adsorption; and
6. a charge neutral, more hydrophobic characteristic of the outer surface and a net negatively charged inner surface [9,10,12].

Electron-microscopic studies revealed that isolated S-layer protein subunits are endowed with the ability to assemble into monomolecular arrays in suspension, on solid phases, at the air/water interface, on liposomes or on lipid films generated by the Langmuir–Blodgett (LB) technique [2,12–14]. The capability of S-layer subunits isolated from different *Bacillus* species to recrystallize on phospholipid- or tetraetherlipid-films led to a new concept of biomimetic membranes (for reviews, see Refs. [13,15]). In particular, S-layer-supported LB-films mimic the structural and functional properties of those archaeobacterial cell en-

velopes which are exclusively composed of a plasma membrane and a closely associated S-layer lattice [3–6,16].

In the present study, S-layer subunits derived from *Bacillus coagulans* E38-66 were recrystallized on a monomolecular film of glycerol dialkyl nonitol tetraether lipid (GDNT) by injecting the subunits into the aqueous subphase. The archaeobacterial membrane-lipid GDNT consists of two branched hydrocarbon chains which are ether-linked at the ends to one glycerol and one nonitol [17,18]. In nature, carbohydrates and phosphoinositols are linked to the nonitol- and glycerol-groups, respectively. Native tetraether lipids are difficult to isolate and to purify in quantities adequate for electrophysical measurements. In the present study, hydrolyzed GDNT was used (Fig. 1) to increase the purity and the amount of usable material [19]. As shown by pressure/area and potential/area isotherms under various subphase conditions, pure LB-films of GDNT form lipid expanded

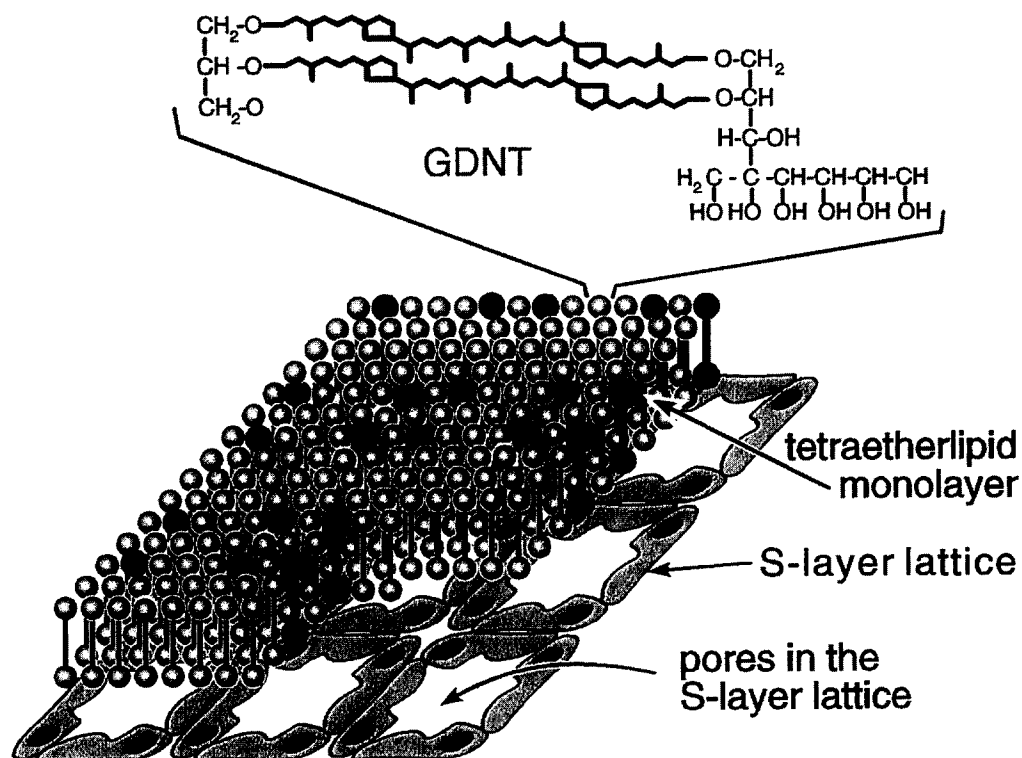


Fig. 1. Schematic illustration of the composite S-layer/GDNT monolayer structure. The chemical structure of the glycerol dialkyl nonitol tetraether lipid (GDNT) molecules is shown at the top of the figure. The black coloured GDNT-molecules represent the most favoured lipids in the GDNT-monolayer, whose associated head groups may interact with defined domains on the S-layer lattice (not drawn to scale).

monolayers [19]. The lipid molecules are arranged in an upright orientation and reveal the dimensions of common phospholipid bilayers [20].

In order to investigate the barrier function and potential to incorporate functional molecules, voltage-clamp examinations on plain and S-layer supported GDNT-monolayers were performed. Valinomycin, a well-described natural antibiotic peptide was used as a model system to measure the ionophore-mediated conductance of the GDNT-monolayer [21,22]. The  $K^+$ -selective cyclodepsipeptide constitutes a threefold repetition of alternating amino-acid and hydroxy-acid residues. Valinomycin in solution exists in a rather complex and flexible set of conformations. From crystallographic data, the cell dimensions of the uncomplexed valinomycin are:  $a = 2.2$  nm,  $b = 1.0$  nm,  $c = 1.5$  nm,  $\alpha = 90^\circ$ ,  $\beta = 105^\circ$  and  $\gamma = 93^\circ$  [22]. Valinomycin is known to show the greatest selectivity for potassium vs. sodium ions in biological studies [22]. It is now widely accepted that one ion is ferried across the membrane by a single carrier molecule [23].

Previous work has demonstrated that S-layer stabilized lipid films (referred to as “semifluid membrane” [24,25]) are able to span holes with a diameter of up to 15  $\mu$ m (for a review, see Ref. [13]). The present study investigates, for the first time, the integrity of an S-layer-supported tetraetherlipid monolayer and the increase in conductance due to the action of valinomycin. Such composite structures may open new ways of exploiting structural and functional principles of membrane-associated and membrane-integrated molecules at meso- and macroscopic scales [13].

## 2. Materials and methods

### 2.1. Formation of the tetraether lipid monolayer

The glycerol dialkyl nonitol tetraether lipid (GDNT; see Fig. 1) was kindly provided by Prof. Heckmann (Institut für Physikalische und Makromolekulare Chemie, Regensburg, Germany) and was dissolved and stored at  $-20^\circ\text{C}$  in chloroform at a concentration of 10 mg lipid/ml solvent. For the generation of the lipid monolayer, a homemade Langmuir–Blodgett (LB) trough with a surface area of

35 cm<sup>2</sup> and two barriers was used. The surface pressure was monitored at 25°C with a homemade Wilhelmy plate apparatus. The LB-trough was filled with 20 ml electrolyte, a drop of solution of GDNT was spread on the air/water interface and compressed to a surface pressure of  $26 \pm 1$  mN/m.

### 2.2. Isolation of S-layer subunits

*Bacillus coagulans* E38-66 was kindly provided by F. Hollaus (Österreichisches Zuckerforschungsinstitut, Tulln, Austria). Growth of the bacteria in continuous culture and cell wall preparations and extraction of S-layer protein with guanidine hydrochloride (GHCl, 5 M in 50 mM Tris hydrochloride buffer, pH 7.2) was performed as previously described [26]. GHCl extracts containing 5 mg protein/ml buffer were dialyzed against  $\text{CaCl}_2$  solution (10 mM in distilled water,  $3 \times 2$  h at 4°C). Subsequently, the S-layer self-assembly products were sedimented for 15 min at  $40\,000 \times g$  at 4°C. The supernatant containing the disassembled S-layer subunits or oligomeric precursors (1.3 mg protein/ml) was used for all recrystallization experiments.

### 2.3. Recrystallization of the S-layer on the GDNT-monolayer

The recrystallization of S-layer subunits on GDNT-monolayers was performed as previously described for phospholipid monolayers [12]. Briefly, after the generation of the GDNT-monolayer, 2 ml of the supernatant of the S-layer solution were carefully injected into the electrolyte subphase (2 mM  $\text{CaCl}_2$ , with 10, 50 or 100 mM KCl, adjusted with citric acid to pH 4.0). Recrystallization of the S-layer subunits on the GDNT/water interface was performed at 25°C overnight. The surface level of the subphase was kept constant within this time by an automatically controlled pump (NFT Level-O-matic, Coventry, UK).

### 2.4. Electron microscopy

The recrystallization of the S-layer protein was monitored by transmission electron-microscopic studies (Philips CM12, Eindhoven, The Netherlands) on negatively stained preparations as previously de-

scribed [7]. The electron-microscope grids, coated with coherent (standard grids) or perforated carbon films (holey grids), were carefully placed onto the composite GDNT/S-layer film and removed after several minutes [24]. Image contrast was enhanced by negative staining of the protein–lipid monolayer with uranyl acetate (2% in distilled water) after fixation with glutaraldehyde (2.5% in 0.1 M cacodylate buffer, pH 7.2) as previously described [12].

### 2.5. Electrophysical measurements

Patch pipettes were pulled from glass capillaries (PG 61165-4, World Precision Instruments, Berlin, Germany) using a vertical puller (Microelectrode Puller Model PB-7, Narishige, Tokyo, Japan). Immediately before use, the tip of the patch pipette was fire-polished on a microforge (Microforge MF-9, Narishige, Tokyo, Japan) to increase the likelihood of generating a tight membrane on the tip. The pipettes, with a tip diameter of 5 to 8  $\mu\text{m}$ , were filled with the same electrolyte as the LB-trough. All solutions were passed through a cellulose acetate filter with 0.2  $\mu\text{m}$  pores (Sartorius AG, Goettingen, Germany). When filled, the pipettes had direct current resistances of 5–10 M $\Omega$ .

The voltage clamp setup was mounted on a steel core breadboard (CS-11-4, Newport, Darmstadt, Germany). The headstage of the patch clamp amplifier (EPC 9, HEKA Elektronik, Lambrecht/Pfalz, Germany) was fixed on a translation stage (M-426, Newport, Darmstadt, Germany) which could be moved vertically (Motorizer 860 A, Newport, Darmstadt, Germany; regulated DC power supply: Kenwood PR 18-1.2, Tokyo, Japan). The headstage of the amplifier, together with the LB-trough, the Wilhelmy system and the sensor of the surface level control unit were placed within a grounded Faraday cage. Both electrodes were made of silver wires (0.4 mm in diameter) covered with AgCl (2 h at 1.5 V DC in a 0.1 N HCl). The reference electrode was connected to the subphase of the LB-trough behind the barrier so as not to interfere with the lipid film. The filled patch pipette was connected to the working electrode and carefully moved against the spread lipid film to generate the GDNT-monolayer on the tip of the patch clamp pipette. Since the glass pipette was moved through the lipid–water interface only once, the

membrane patch, sealing the tip, must have been a monolayer. In some experiments, after the GDNT-monolayer had been generated on the tip of the glass pipette, S-layer subunits were injected into the subphase of the LB-trough and the protein was allowed to recrystallize on the lipid monolayer. In some experiments, the recrystallized S-layer protein was cross-linked by injecting glutaraldehyde (25% solution in the subphase buffer) into the subphase of the GDNT/S-layer film. The final concentration of glutaraldehyde in the subphase was 1.25%. Valinomycin (Sigma, Deisenhofen, Germany) was injected with a syringe (Hamilton Microliter Syringe, Bonaduz, Switzerland) from an ethanolic stock ( $10^{-5}$  M) underneath the preformed GDNT-monolayer or GDNT/S-layer film (final valinomycin concentration was  $10^{-7}$  M). The content of ethanol was kept very low and found not to interfere with pore formation or changing the conductance of the membranes.

### 2.6. Signal recording and data acquisition

The current response of a given voltage function was measured at 25°C to calculate the electrophysical parameters of plain and S-layer-supported GDNT membranes. Capacitance measurements were carried out using a triangular 40 mV function with a peak-to-peak interval of 40 ms. The contribution of the glass pipette to the measured capacitance was determined. For this reason, glass pipettes, filled with electrolyte were pressed against Sylgard (Dow Corning Corporation, Midland, MI) and, subsequently, allowed to cure at room temperature. The determination of the capacitance was carried out in the same way as already described. Conductance was measured via a 200 or a 25 ms rectangular voltage pulse of 40 mV across the membrane. All the data handling (voltage stimulation, data acquisition, data storage, data analysis) was performed on a Mac II vx personal computer (Apple Computer GmbH, Ismaning, Germany). The setting of the two built-in Bessel filters of the EPC 9 amplifier for the current-monitor signal was 10 and 2.9 kHz, respectively. The data analysis was performed by the Pulse + PulseFit software 7.89/Quadra (HEKA Elektronik, Lambrecht/Pfalz, Germany). Correlations of conductance vs. time and statistical analysis (ANOVA) were performed by using the Jandel SIGMA PLOT program for Windows.

### 3. Results

In the present study, the concentration of potassium ions in the electrolyte in the trough needed to be optimized in order to find conditions suitable for both the recrystallization of the S-layer protein on GDNT-monolayers and for studying the valinomycin-mediated increase in conductance of the plain and S-layer supported GDNT-monolayer. No detectable difference was observed in the spreading characteristics of GDNT-monolayers and the subsequent seal formation between the glass of the patch pipette and the lipid film in the presence of 10 to 100 mM KCl. On the other hand, the KCl concentration exerted a pronounced influence on the recrystallization of the S-layer protein on the GDNT-monolayer as determined by transmission electron microscopy. Using an electrolyte containing 100 or 50 mM KCl, only a few separated patches of recrystallized S-layer protein were observed.

Recrystallization of S-layer protein on the GDNT-monolayer into coherent layers only occurred when the concentration of KCl was lowered to 10 mM. Thus, for all further experiments an electrolyte containing 10 mM KCl, 2 mM  $\text{CaCl}_2$ , pH 4.0 was used.

#### 3.1. Recrystallization of the S-layer on the GDNT-monolayer

Electron-microscopic studies showed that the S-layer recrystallization process on GDNT-monolayers was initiated at several distant nucleation points (Fig. 2(A)) and terminated locally when the advancing front regions of neighboring crystalline areas had met. As demonstrated in previous recrystallization studies on dipalmitoylphosphatidylcholine and dipalmitoylphosphatidylethanolamine monolayer films

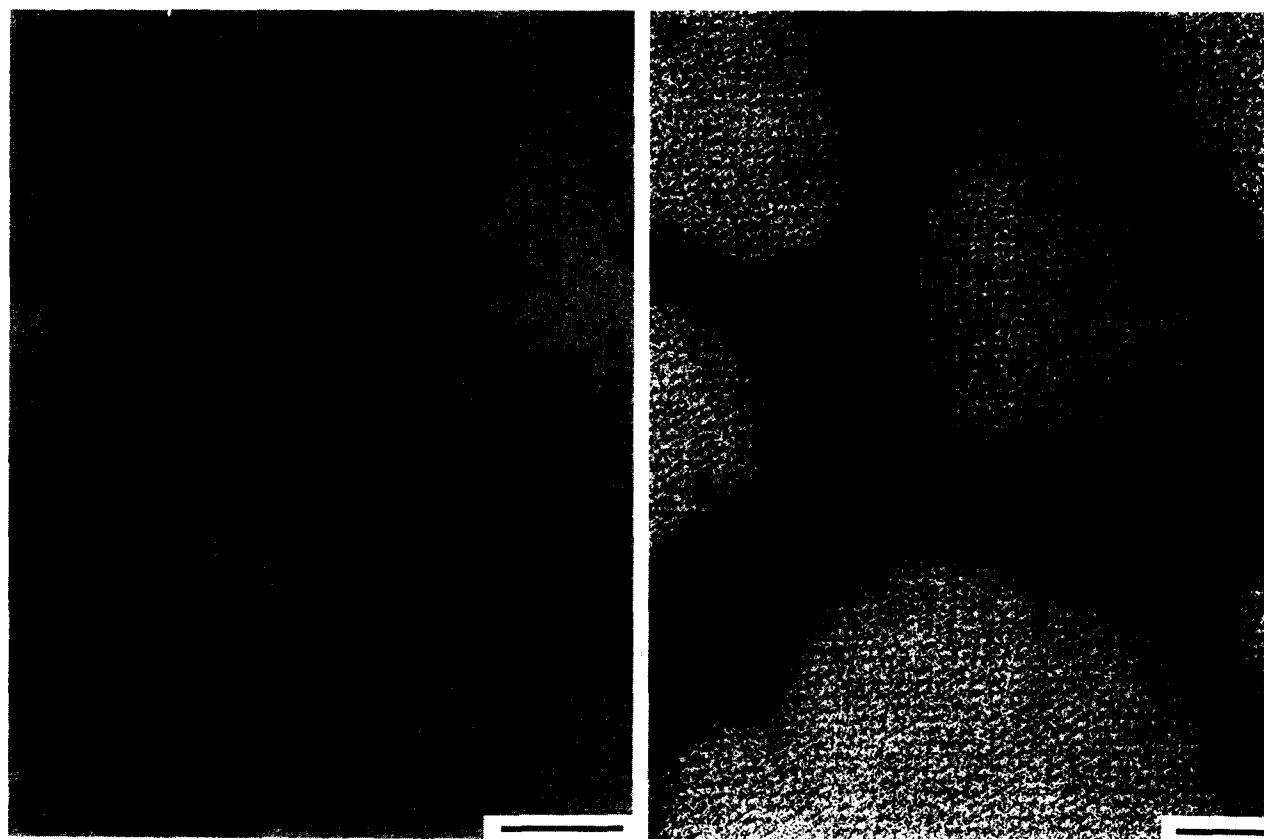


Fig. 2. Electron micrographs of negatively stained preparations illustrating the crystallization process of S-layer subunits isolated from *B. coagulans* E38-66, recrystallized on a glycerol dialkyl nonitol tetraether lipid (GDNT) monolayer. (A) Crystal growth is initiated at several distant nucleation points. The scale bar represents 1  $\mu\text{m}$ . (B) A monomolecular coherent S-layer recrystallized on a GDNT monolayer covers completely a holey electron microscope grid. The scale bar represents 0.1  $\mu\text{m}$ .

[12], no overlaps at the boundary lines could be observed. A comparison of the handedness between the oblique S-layer lattice on freeze-etching preparations of whole bacterial cells [10] and the S-layer recrystallized on GDNT-monolayers revealed that the S-layer was attached to the lipid film with its outer surface. Although S-layer recrystallization was generally completed after 3.5 h, most voltage clamp studies were performed after a recrystallization overnight. After injection of S-protein monomers underneath the GDNT-monolayer, an increase in surface pressure was observed: from  $26 \pm 1$  mN/m initially to  $32 \pm 1$  mN/m ( $n = 6$ ). This observed change in surface pressure indicated an interaction of lipid head groups in the GDNT-monolayer with defined domains of the S-layer lattice (Fig. 1). Subsequent electron-microscopic inspections of negatively stained preparations showed that monolayers of the S-protein were formed and that two-dimensional crystals with oblique lattice symmetry were grown. As shown in Fig. 2(B), S-layer-supported GDNT-monolayers (schematically depicted in Fig. 1) are able to span even large openings of holey electron-microscope grids.

### 3.2. Voltage clamp measurements on plain and S-layer supported GDNT-monolayer

The patch pipette was moved towards the GDNT-monolayer and a seal formation between the glass of the patch pipette and the lipid film occurred. The resistance increased from 5–10 M $\Omega$  (plain patch pipette) upon formation of the lipid membrane on the tip of the glass pipette instantaneously in the giga-ohm range. Thus, the GDNT-monolayer tightly sealed the glass pipette in the same manner as it has already been reported for phospholipids [27]. In more than 80% a lipid monolayer could be generated on the tip of the glass pipette at the first trial. Whenever the second trial was not successful, the pipette was displaced by a new one. In comparison, the plain GDNT-monolayer displayed a higher conductance ( $11.0 \pm 7.0$  pS, corresponding to  $22.0 \pm 14.0$   $\mu$ S/cm $^2$ ;  $n = 5$ ) than the S-layer-supported lipid film ( $4.7 \pm 4.0$  pS, corresponding to  $9.4 \pm 8.0$   $\mu$ S/cm $^2$ ;  $n = 5$ ). The main contribution to the measured capacitance was found to come from the glass pipette as determined with a glass pipette whose tip had been closed with Sylgard ( $5.2 \pm 0.3$  pF;  $n =$

8). Nevertheless, the capacitance of the glass pipette with the plain ( $5.6 \pm 0.3$  pF;  $n = 5$ ) and the S-layer-supported GDNT-monolayer ( $5.4 \pm 0.3$  pF;  $n = 5$ ) sealing the tip was also measured. The contribution of the glass pipette to the measured capacitances was subtracted and resulted in 0.4 and 0.2 pF for the plain and S-layer-supported GDNT-monolayers, respectively. This corresponded to 0.8  $\mu$ F/cm $^2$  for the plain and to 0.4  $\mu$ F/cm $^2$  for the S-layer supported GDNT-monolayer.

### 3.3. Voltage clamp measurements on plain and S-layer-supported GDNT-monolayer with incorporated valinomycin

An addition of the K $^+$ -ion selective ion-carrier valinomycin into the subphase of the preformed plain or S-layer-supported GDNT-monolayer caused an increase of the measured transmembrane current leading to an increase of the calculated conductance when a certain potential was applied. This current response was only observed with K $^+$ -ions but not when they were replaced by Na $^+$ -ions (data not shown). Thus, the increase in conductance was clearly due to the specific carrier function of valinomycin. These results also indicated that valinomycin was incorporated not only in plain but also in S-layer-supported GDNT-monolayers (Fig. 3). Upon addition of valinomycin to plain GDNT-monolayers, the membrane gained max-

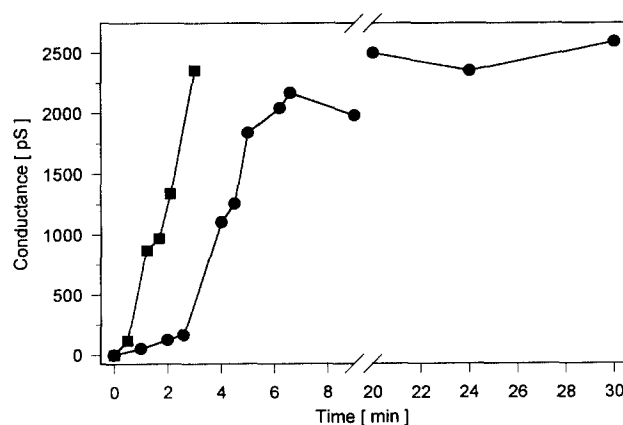


Fig. 3. A typical experimental run indicating the time-dependent conductance for a (■) plain and (●) S-layer-supported glycerol dialkyl nonitol tetraether lipid (GDNT) monolayer after the addition of the ion-carrier valinomycin to the subphase of the Langmuir–Blodgett trough (final concentration  $10^{-7}$  M). The conductance was calculated from the transmembrane current after a voltage step of 40 mV.

imum conductance ( $2570 \pm 520$  pS,  $n = 5$ ; corresponding to  $5140 \pm 1040$   $\mu\text{S}/\text{cm}^2$ ) within a short time. Rupture of the plain GDNT-monolayer was observed after 3–4 min. The maximum increase of the conductance, estimated by the slope of the conductance–time plot (Fig. 3) was calculated at 1020 pS/min. A significantly different response was observed upon adding valinomycin to S-layer-supported GDNT-monolayers (Fig. 3). The conductance of the membrane increased only moderately within 3 min after the addition of valinomycin. Subsequently, the conductance rose with a maximum increase of 663 pS/min, reaching a conductance of  $\sim 2000$  pS ( $4000$   $\mu\text{S}/\text{cm}^2$ ) after 10–15 min. During the subsequent 20 min, the conductance increased only slowly up to  $2600 \pm 670$  pS,  $n = 5$ ; corresponding to  $5200 \pm 1340$   $\mu\text{S}/\text{cm}^2$ . A rupture of the S-layer-supported GDNT-monolayer was generally observed after 30 min. Cross-linking the S-layer protein from the subphase with glutaraldehyde affected no significant difference in the measured electrophysical parameters with, and without valinomycin (data not shown).

#### 4. Discussion

While recrystallization of various S-layers on many different phospholipids has been previously demonstrated by electron-microscopic investigations [12,13,24], no evidence concerning the structural and functional integrity of such composite supramolecular structures has been provided.

The aim of the present study is to assess the electrophysical features of S-layer-supported GDNT-monolayer on the tip of a patch pipette. To our knowledge, a biomimetic archaeobacterial cell envelope built of an S-layer-supported GDNT-monolayer (Fig. 1) has never been previously studied in this manner. In comparison to black lipid membranes spanning Teflon apertures [20], the calculated specific conductance ( $22.0 \pm 14.0$   $\mu\text{S}/\text{cm}^2$ ) measured for plain GDNT-monolayers was relatively high. On the other hand, a comparison of the measured resistance of the GDNT-monolayer with phospholipid bilayers generated by the “tip-dip” method [27] showed similar results.

Upon recrystallization of S-layer protein, a significant increase of the surface pressure was observed.

However, as previously demonstrated at even higher surface pressure, the GDNT-monolayer behaved as a lipid expanded film [19]. A similar increase in surface pressure upon S-layer recrystallization was found for many phospholipid-monolayers (unpublished results). These observations were explained by a substantial increase in segmental order of the lipid chains due to noncovalent interactions between the lipid film and defined domains of the S-layer protein without interpenetration of the absorbent protein molecules into the lipid monolayer [28]. It seems very unlikely that the protein could interpenetrate into the lipid film without destroying the lipid monolayer structure [28]. The results of the voltage clamp studies indicate that, upon recrystallization of the S-layer protein on the GDNT-monolayer, the integrity of the lipid film was not disturbed. Such disturbance would have resulted in a dramatic increase in conductance of the membrane. The observed decrease in membrane conductance, following recrystallization of the S-layer lattice from  $22.0 \pm 14.0$  to  $9.4 \pm 8.0$   $\mu\text{S}/\text{cm}^2$ , constitutes evidence for the composite membranes being less permeable for charged molecules than plain GDNT-monolayers.

A calculation of the specific capacitance of the membranes from the measured signal was hardly feasible since the contribution of the glass pipette to the measured capacitance was found to be very large. Two possible sources of errors, different depths of immersion of the glass pipette and covering the outer surface of the tip region of the pipette with Sylgard, might seriously interfere with the calculation of the membrane capacitance [29]. However, the capacitance of the glass pipettes with Sylgard-sealed tips was subtracted from the measured signal to estimate the capacitance of the clamped membranes [29]. The specific capacitance of the plain GDNT-monolayer was found to be  $0.8$   $\mu\text{F}/\text{cm}^2$ . This is in good agreement with the previously reported value of  $0.7 \pm 0.08$   $\mu\text{F}/\text{cm}^2$  for GDNT-monolayers formed on Teflon septa [30]. GDNT/S-layer-membranes showed a lower specific capacitance ( $0.4$   $\mu\text{F}/\text{cm}^2$ ). A previous study also similar specific capacitances for some GDNT-membranes [30]. As the corresponding mean dielectric thickness is higher than the fully extended length of the hydrocarbon chain of one GDNT-molecule, they suggested an n-shaped configuration of the GDNT-molecules, which would form a double layer.

However, these GDNT-membranes were formed using a huge amount of GDNT and, thus, most probably out from multilayers. In the present study, the GDNT-monolayer was formed by the LB-technique. Lipid molecules were compressed from the “gas”-state to form the GDNT-monolayer. Furthermore, LB-studies on GDNT-monolayers showed no evidence for such n-shaped structures [19]. Additionally, a similar increase in surface pressure upon S-layer protein recrystallization has been observed for both, GDNT- and phospholipid-monolayers (unpublished observations). Thus, it is unlikely that a substantial protein-induced change of the lipid molecules from an upright to an n-shaped configuration occurred. Another explanation would be that the attached protein layer increased the hydrophobic thickness of the membrane or changed the capacitance of the Gouy–Chapman–Stern layer [31]. Impedance measurements or spectroscopical methods could help to elucidate this question.

Monolayers generated from GDNT have already been shown to form suitable matrices for the functional incorporation of lipid active proteins [32,33]. In the present study, the  $K^+$ -selective ion-carrier valinomycin was incorporated into a plain- and an S-layer-supported GDNT-monolayer in order to compare the increase in conductance of both membranes.

The conductance of the unsupported GDNT-monolayer increased in the presence of valinomycin within a few minutes to a maximal value. In black lipid membranes composed of tetraether lipids, particularly GDNT, valinomycin mediated a higher specific conductance than in membranes composed of phospholipids [20]. However, similar specific conductances were measured under comparable conditions for phosphatidyl inositol membranes in the presence of valinomycin [34]. The time course of the valinomycin-mediated conductance and its final value depend, in case of black lipid membranes, on the relative magnitude of two total valinomycin fluxes, namely from water to membrane and from membrane into the torus (Plateau–Gibbs–Border) [35]. A smaller flow of valinomycin into the torus compared with the total valinomycin flux from the aqueous phase into the membrane leads to a higher specific conductance of black lipid membranes [35]. Less is known about the nature of the interaction of the lipid with the glass surface of the pipette, leading to the observed tight

seal [29]. However, neither a pretreatment of the orifice with alkane [20], nor a huge excess of lipid [30] was necessary to generate the GDNT-monolayer on the glass pipette by the “tip-dip”-method; it is therefore very unlikely that the lipid forms a torus towards the glass rim of the pipette. Thus, exchange of valinomycin occurred only between membrane and water. The observed strong increase in conductance and the high final specific conductance compared with black lipid membranes (Fig. 3) may reflect the higher amount of valinomycin acting as ion-carrier, as no loss of uncomplexed valinomycin occurred by the permanent flow of the valinomycin from the membrane into the torus.

The voltage clamp measurements on the S-layer-supported GDNT-monolayer showed a valinomycin-mediated increase in conductance. The time-dependent changes in conductance upon incorporation of valinomycin indicate significant differences between the plain and the S-layer-supported GDNT membrane (Fig. 3). Although, in comparison to plain GDNT-monolayers, a slower increase in valinomycin-mediated specific conductance was observed for GDNT/S-layer membranes, the final conductance was almost identical in both systems. These results indicated free passage of valinomycin through the S-layer lattice to the lipid membrane. Both, high resolution electron-microscopic and permeability studies [9,11,12] have demonstrated that pores with a diameter of 3.5 nm are present in the S-layer lattice of *Bacillus coagulans* E38-66. Previous permeability studies on these S-layer lattices [9] showed free passage for myoglobin (molecular size  $2.5 \times 3.5 \times 4.5$  nm). Thus, the pores of the S-layer lattice must be too large to hinder the passage of valinomycin ( $2.2 \times 1.0 \times 1.5$  nm; [22]). Moreover, ultrafiltration membranes composed of *B. coagulans* E38-66 as permselective layer [9,11] allowed the free passage of valinomycin without any measureable solute rejection (unpublished observation). These data do not completely exclude the fact that, to a certain extent, the S-layer lattice may impede the diffusion of valinomycin to the attached GDNT-monolayer. The slower increase in conductance observed for the GDNT/S-layer membrane may also be explained by the influence of the S-layer lattice on the lipid monolayer. According to the “semifluid-membrane”-model [25] a proportion of lipid head groups in the monolayer



film is expected to interact in a well-defined way with domains of the associated protein lattice (Fig. 1), inducing an enhanced order of the alkane chains of the lipid molecules [13,24,28]. Temperature-induced structural changes of black lipid membranes were probed by the use of valinomycin [36]. The observed decrease of the conductance with decreasing temperature was interpreted by a decreased fluidity of the lipid molecules within the membrane. Since the fluidity of lipid membranes is known to have a strong effect on the functionality of integral membrane proteins [37] it can be assumed that the more rigid, S-layer-supported lipid matrix is responsible for the observed slower incorporation of valinomycin and/or complexation of  $K^+$ -ions by valinomycin. Finally, the S-layer-supported GDNT-monolayer revealed approximately the same valinomycin-mediated conductance as the unsupported GDNT-monolayer, but the former showed no rupture over at least 25 min. This observation might indicate that the attachment of an S-layer led to an enhanced stability of the clamped GDNT-monolayer with incorporated valinomycin molecules. However, it was not the aim of the present study to present kinetic data on the action of valinomycin. This work is the first attempt to characterize and make use of S-layer-supported lipid membranes. Further studies are in progress to exploit these composite lipid/S-layer structures.

In conclusion, S-layer-supported lipid membranes provide an interesting biomimetic matrix with adequate flexibility and stability for electrophysical studies. These properties are the basis of a new approach to the study of lipid–protein interactions and the function of membrane-associated or membrane-integrated biomolecules. Since electron-microscopic studies have demonstrated that S-layer-supported lipid membranes can cover apertures up to 15  $\mu\text{m}$  diameter [13,24], such biomimetic functional membranes may be exploited at meso- or macroscopic scale not only by electrophysical methods but also by electron or scanning force microscopy [14].

### Acknowledgements

We thank H. Ti Tien and F.M. Unger for critical reading of the manuscript and S. Zayni and A. Scheberl for their technical assistance. This work was

supported by grants from the Austrian Science Foundation, Projects S7204 and S7205, the Austrian National Bank, Project 5525 and the Austrian Federal Ministry of Science, Transport and the Arts.

### References

- [1] U.B. Sleytr, *Int. Rev. Cytol.* 53 (1978) 1–64.
- [2] U.B. Sleytr, P. Messner, D. Pum, M. Sára, in: U.B. Sleytr, P. Messner, D. Pum, M. Sára (Eds.), *Crystalline Bacterial Cell Surface Layers*, Springer-Verlag, Berlin, 1988.
- [3] U.B. Sleytr, P. Messner, D. Pum, M. Sára, *Mol. Microbiol.* 10 (1993) 911–916.
- [4] U.B. Sleytr, P. Messner, D. Pum, M. Sára, in: U.B. Sleytr, P. Messner, D. Pum, M. Sára (Eds.), *Crystalline Bacterial Cell Surface Proteins*, Proteins Academic Press, Austin, TX, 1996.
- [5] P. Messner, U.B. Sleytr, in: A.H. Rose (Ed.), *Advances in Microbiol. Physiology*, Vol. 33, Academic Press, London, 1992, pp. 213–275.
- [6] W. Baumeister, H. Engelhardt, in: J.R. Harris, R.W. Horne (Eds.), *Electron Microscopy of Proteins*, Academic Press, London, 1987, p. 109.
- [7] D. Pum, M. Sára, U.B. Sleytr, *J. Bacteriol.* 171 (1989) 5296–5303.
- [8] T.J. Beveridge, *Curr. Opin. Struct. Biol.* 4 (1994) 202–212.
- [9] M. Sára, D. Pum, U.B. Sleytr, *J. Bacteriol.* 174 (1992) 3487–3493.
- [10] M. Sára, U.B. Sleytr, *J. Bacteriol.* 175 (1993) 2248–2254.
- [11] M. Sára, U.B. Sleytr, in: H.-J. Rehm (Ed.), *Biotechnology*, Vol. 6b, VCH, Weinheim, 1988, pp. 615–636.
- [12] D. Pum, M. Weinhandel, C. Hödl, U.B. Sleytr, *J. Bacteriol.* 175 (1993) 2762–2766.
- [13] D. Pum, U.B. Sleytr, in: U.B. Sleytr, P. Messner, D. Pum, M. Sára (Eds.), *Crystalline Bacterial Cell Surface Proteins*, Academic Press, Austin, Texas, 1996, pp. 175–209.
- [14] B. Wetzler, D. Pum, U.B. Sleytr, *J. Struct. Biol.* 119 (1997) 123–128.
- [15] M. Sára, U.B. Sleytr, *Progr. Biophysics Mol. Biol.* 65 (1996) 83–111.
- [16] H. König, *Can. J. Microbiol.* 34 (1988) 395–406.
- [17] Y. Koga, M. Nishihara, H. Morii, M. Akagawa-Matsushita, *Microbiol. Rev.* 57 (1993) 164–182.
- [18] F. Paltauf, *Chem. Phys. Lipids* 74 (1994) 101–139.
- [19] J.L. Dote, W.R. Barger, F. Behroozi, E.L. Chang, S.-L. Lo, C.E. Montague, M. Nagumo, *Langmuir* 6 (1990) 1017–1023.
- [20] J. Stern, H.J. Freisleben, S. Janku, K. Ring, *Biochim. Biophys. Acta* 1128 (1992) 227–236.
- [21] P. Läger, *J. Membr. Biol.* 57 (1980) 163–178.
- [22] M. Dobler, in: *Ionophores and Their Structures*, Wiley Interscience Publication, New York, 1981, pp. 39–51.
- [23] S.B. Hladky, J.C.H. Leung, W.J. Fitzgerald, *Biophys. J.* 69 (1995) 1758–1772.
- [24] D. Pum, U.B. Sleytr, *Thin Solid Film* 244 (1994) 882–886.

- [25] U.B. Sleytr, M. Sára, P. Messner, D. Pum, J. Cell. Biochem. 56 (1994) 171–176.
- [26] U.B. Sleytr, M. Sára, Z. Küpcü, P. Messner, Arch. Microbiol. 146 (1986) 19–24.
- [27] R. Coronado, R. Latorre, Biophys. J. 43 (1983) 231–236.
- [28] A. Diederich, C. Hödl, D. Pum, U.B. Sleytr, M. Lösche, Coll. Surf. B 6 (1996) 335–343.
- [29] B. Sakmann, E. Neher, in: B. Sakmann, E. Neher (Eds.), Single-Channel Recordings, Plenum Press, New York, 1995, pp. 637–650.
- [30] A. Gliozzi, M. Robello, A. Relini, G. Accardo, Biochim. Biophys. Acta 1189 (1994) 96–100.
- [31] M. Stelzle, G. Weissmüller, E. Sackmann, J. Phys. Chem. 97 (1993) 2974–2981.
- [32] M.G.L. Elfterink, J.G. de Wit, R. Demel, A.J.M. Driessen, W.N. Konings, J. Biol. Chem. 267 (1992) 1375–1381.
- [33] M.G.L. Elfterink, T. Bosma, J.S. Lolkema, M. Gleiszner, A.J.M. Driessen, W.N. Konings, Biochim. Biophys. Acta. 1230 (1995) 31–37.
- [34] G. Stark, R. Benz, J. Memb. Biol. 5 (1971) 133–153.
- [35] R. Benz, G. Stark, K. Janko, P. Läuger, J. Membr. Biol. 14 (1973) 339–366.
- [36] G. Stark, R. Benz, G.W. Pohl, K. Janko, Biochim. Biophys. Acta 266 (1972) 603–612.
- [37] E. Sackmann, in: R. Lipowsky, E. Sackmann (Eds.), Structure and Dynamics of Membranes, Elsevier, Amsterdam, 1995, pp. 213–304.